

## On the effect of porosity on the shear correction factors of functionally graded porous beams

Ben Abdallah Medjdoubi<sup>1</sup>, Mohammed Sid Ahmed Houari\*<sup>1</sup>, Mohamed Sadoun<sup>1</sup>,  
Aicha Bessaim<sup>1</sup>, Ahmed Amine Daikh<sup>1,2</sup>, Mohamed-Ouejdi Belarbi<sup>3</sup>,  
Abdelhak Khechai<sup>3</sup>, Aman Garg<sup>4</sup> and Mofareh Hassan Ghazwani<sup>5</sup>

<sup>1</sup>Laboratoire d'Etude des Structures et de Mécanique des Matériaux, Département de Génie Civil,  
Faculté des Sciences et de la Technologie, Université Mustapha Stambouli, Mascara 29 000, Algérie

<sup>2</sup>Department of Technology, University Centre of Naama, P.O. Box 66, 45000 Naama, Algeria

<sup>3</sup>Laboratoire de Recherche en Génie Civil, LRGCC, Université de Biskra, B.P. 145, R.P. 07000, Biskra, Algeria

<sup>4</sup>Department of Civil and Environmental Engineering, The NorthCap University,  
Gurugram, Haryana, 122017, India

<sup>5</sup>Department of Mechanical Engineering, Jazan University, P.O. Box 114, Jazan, 45142, Saudi Arabia

(Received October 12, 2022, Revised May 3, 2023, Accepted May 4, 2023)

**Abstract.** This article presents a new analytical model to study the effect of porosity on the shear correction factors (SCFs) of functionally graded porous beams (FGPB). For this analysis, uneven and logarithmic-uneven porosity functions are adopted to be distributed through the thickness of the FGP beams. Critical to the application of this theory is a determination of the correction factor, which appears as a coefficient in the expression for the transverse shear stress resultant; to compensate for the assumption that the shear strain is uniform through the depth of the cross-section. Using the energy equivalence principle, a general expression is derived from the static SCFs in FGPB. The resulting expression is consistent with the variationally derived results of Reissner's analysis when the latter are reduced from the two-dimensional case (plate) to the one-dimensional one (beam). A convenient algebraic form of the solution is presented and new study cases are given to illustrate the applicability of the present formulation. Numerical results are presented to illustrate the effect of the porosity distribution on the (SCFs) for various FGPBs. Further, the law of changing the mechanical properties of FG beams without porosity and the SCF are numerically validated by comparison with some available results.

**Keywords:** functionally graded beam; porosity; shear correction factor; transverse shear

### 1. Introduction

From the turn of the 20th century to the present day, the engineering design of composites for structural applications requires higher strength-to-weight and stiffness-to-weight ratios involved in manufacturing processes. Nevertheless, the problem of developed stress concentrations at the interfaces between the layers constitutes a major drawback. In order to have an important

---

\*Corresponding author, Professor, E-mail: ms.houari@univ-mascara.dz

characteristic of composite materials such as the elimination of delamination and cracking; in the mid-1980s Japanese researchers designed new materials called, Functionally Graded Materials (FGMs). However, this concept was proposed by Bever and Duwez (1972) and by several researchers in the United States (Goetzel and Lavendel 1964). Its exploitation in composite materials was tried sporadically in the 1950s, 1960s, 1970s, and 1980s. However, these studies had a limited impact at that time due to the lack of a design, a manufacturing method, and a method for evaluating graded structures. These initial estimates of the advantage of FGMs consist of a variety of material properties from one surface to another according to specific mathematical rules in chosen directions providing a continuous stress distribution in the FGM structure. For this reason, they are classed as advanced composite materials, which attracted many research organizations, (Koizumi 1997, Suresh and Mortensen 1998). These organizations focused their researchers on structures subjected to cold conditions on one side and to very hot environment on the other. Thus, various methods have been developed to manufacture the FGMs such as High-speed centrifugal casting; Ultraviolet irradiation process and direct oxidation technique, etc. A number of investigations have been made on FGM beams and plates to study their static and dynamic behaviours. Plates are the commonly used structural members that have numerous applications in aerospace industries, civil and mechanical engineering.

Functionally graded porous (FGP) materials are an example of innovative development in the materials industry and are engineered for use in many sectors. Their reputation comes from their high surface area to volume ratio of consolidating phase. Nowadays, FGP nanocomposite materials are produced by adding carbon nanotubes (CNTs) and graphene platelets (GPLs) on a nanoscale level to metal, ceramic, or polymer matrices. This addition improves the energy absorption properties of thin-walled rings, arches, beams, and plates considerably. These materials are commonly chosen for a wide range of engineering applications, including lightness, electrical conductivity, energy absorption, and thermal management. FGP materials have unique physical and materialistic properties resulting from their composition or microstructure shape, which is specifically adjusted to meet the needs of particular operations. The development of FGPs aimed to reduce stress fluctuations in composite materials, and they exhibit decreased transverse and in-plane stresses, minimized residual stress, elevated thermal resistance, minimized thermal conductivity, and elevated fracture toughness and resistance to interlaminar stresses from an engineering perspective.

However, a detailed analysis conducted by Yas and Rahimi (2020) on FGP nanocomposites, specifically on weight fraction, scattering patterns, size and geometry of platelets, and porosity allocation and coefficient, revealed that the operation performance of graphene platelets (GPLs) depends heavily on their geometry. Yas and Rahimi (2020) presented free vibration, buckling, and bending analysis of FG graphene nanoplatelets (GNPs)-reinforced nanocomposites under hygro-thermo-mechanical loads. The results showed that the assembly becomes stiffer as the weight fraction of GNPs increases, leading to an increase in the natural frequency and critical buckling stress. However, elevated temperature and moisture decrease the stiffness, natural frequency, and critical buckling load (Jalali *et al.* 2019). Safaei *et al.* (2019) investigated the effects of CNTs and porosity properties of CNT cluster/polymer porous nanocomposite sandwich plates (PNSPs) and examined the mechanical and thermal stresses, geometry, elastic foundation parameters, and boundary conditions that impact the loading distributions and bending of PNSPs. The authors found that functional grading of the core decreases deflection, and the utilization of 5% volume fraction CNTs has negligible impact on the deflection of PNSPs due to the growth of CNT clusters.

Various plate theories have been proposed by researchers to study the bending, buckling, and free vibration behaviours of thin and thick FG plates. Due to its high efficiency and simplicity, the first-order shear deformation theory (FSDT) was used for analyzing moderately thick FG plates. Several authors have proposed models that take into account the transversal shear effect. Based on the Classical laminate theory CPT, FSDT, and third-order shear deformation plate theory (TSDT), a comprehensive work on the free vibration, buckling, and static deflections of FG square, circular, and skew plates, with different combinations of boundary conditions, was carried out by Abrate (2006). Ferreira *et al.* (2006) employed the collocation method with multiquadric radial basis functions along with the FSDT and TSDT to find natural frequencies of FG square plates with different boundary conditions. Zhao *et al.* (2009) presented a free vibration analysis for FG square and skew plates with different boundary conditions using the element-free KP-Ritz method using the FSDT.

The necessary term, used in the FSDT, is the SCF which amends the effect of uniform transverse stress in shear forces, who is mainly equal to  $5/6$  in isotropic homogeneous plates. Noor *et al.* (Noor *et al.* 1989, 1990) proposed predictor-corrector procedures to correct the SCF by using an iteration process. The SCFs obtained from this method depend on boundary conditions, plate geometry, and loading conditions, and hence, they cannot be directly applied to other plate configurations. The introduction of energy considerations in composite laminates, in order to calculate the SCFs, can be found in (Whitney 1973, Bert 1973, Vlachoutsis 1992, Berthelot 1992) presented for composite beams a simplified analysis of the static SCF by the derivation of its expression for laminated cross-ply beams. Whitney (Whitney 1973) presented results from this analysis. By comparing the shear strain energy with the equivalent Timoshenko beam, Bert and Gordaninejad (1983) developed a closed-form solution for the laminated beam.

Birman and Bert (2002) have made an important review and discussion of the philosophies and results of determining SCF for homogeneous rectangular cross-sections as well as the case of sandwich structures. Based on consistent kinematic assumptions of Timoshenko beam theory, Madabhushi-Raman and Davalos (1996) are presented an engineering approach including the transverse shear deformation, in the formulation of the mechanics of laminated beams (MLB) of rectangular beam.

The material properties in FG plates vary along the thickness direction, in practice and due to the use of constant SCF errors in the results occur; Timoshenko showed that the SCF depends on the Poisson's ratio (Timoshenko 1922). Recently, many studies have been done on the formulation of SCF in FGM plates. Efraim and Eisenberger (2007) considered the volume fractions and Poisson's ratio of the two gradients. Nguyen *et al.* (2006) used FSDT to model power-law function gradient material (P-FGM) structures by presenting this factor in terms of ceramic-to-metal Young's modulus ratio, and gradient indices to examine the static analysis.

Some researchers have tried to improve these factors to get results that are more accurate for plate vibration. In general, the FSDT are used to determine the transverse shear strain through the thickness. The accuracy of FSDT is influenced by the accuracy of the SCF used in the theory to calculate the transverse shear forces. Most studies have focused on deriving SCFs for composite laminated beams and very little effort has been devoted to deriving SCFs for functionally graded beams (FGB). A formula is derived from an energy equivalence principle, and the integral equation is simplified into a convenient algebraic form, which reduces to the common expression for isotropic materials reported in the literature. In addition, the study of the effect of the on the static response of the plates can be found in the studies presented by Chi and Chung (2006) and Nguyen *et al.* (2006).

In order to understand the static and dynamic behavior of structures made of FGM, taking into account the effect of porosity, various interesting studies have been developed by Reddy (2002), Wattanasakulpong *et al.* (2014), Mouaici *et al.* (2016), Saidi *et al.* (2019), Merdaci *et al.* (2019).

On the other hand, various recent theoretical developments have been investigated the FGM porous structures. Chen *et al.* (2016) are studied the elastic buckling and bending response of a porous FG beam based on the Timoshenko beam theory. In addition, Chen *et al.* (2016) investigated the nonlinear free vibration of a porous sandwich core with an FG beam. The free vibration and flexural response of porous plates supported by different types of boundary constraints were analyzed by Rezaei and Saidi (2015, 2016, 2017). A quasi-3D shear deformation theory was used to examine the static response of porous FGM single-layered and sandwich plates by Zenkour (2018). The free vibration and bending analysis of Levy type porous FGM plates were investigated Demirhan and Taskin (2019). In a thin S-FGM plate based on the nonlinear CPT model, Wang and Zu (2017) introduced two types of porosity distribution, using the Galerkin method in vibration analysis. Singh and Harsha (2020b) studied the effect of porosity and temperature on sandwich S-FGM plate. The research in the field of FGM plate with porosity effect and elastic foundation remains limited. Unlike the conventional FSDT and the higher-order shear deformation theories, Sadoun *et al.* (2014) proposed a new simple FSDT which contains only four unknowns. They concluded that the proposed theory is precise and simple to solve the static bending and free vibration behaviours of laminated composite plates and the analytical solutions of simply supported antisymmetric cross-ply and angle-ply laminates are accurate compared with the exact three dimensional (3D) solutions. The determination of the transverse SCF poses a problem to compensate for the assumption that the shear strain is uniform throughout the depth of the cross-section. Meena *et al.* (2012) presented a general expression for evaluating these factors (SCF) for general FGM rectangular beams. The SCF of FG beams is not the same as that of homogeneous beams and it is a function of the ratio between the elastic moduli of the constituents and the material parameter  $p$ . The SCF of sigmoid FGMs (S-FG) beams is slightly lower than that of power-law (P-FG) beams when the material parameter  $p$  is less than unity ( $p < 1$ ) and for the material parameter  $p$  greater than unity ( $p > 1$ ). The SCF of the P-FG beam is lower than that of the S-FG beam, unlike the case where  $p < 1$ .

This paper aims to study the effect of porosity on the SCF of the FG porous beam using a new analytical model. Uneven porosity and logarithmic uneven distribution through the thickness of the FGPB are selected here for the analysis. Several parameters such as thickness ratios, volume fractions, and types of distribution are also investigated.

## 2. Model and theoretical formulations

### 2.1 Material gradient of FGP FGP beam

We consider the FGP Beam (see Fig. 1) with the geometry parameter: thickness  $h$ , length  $L$ , and width  $b$  made from the mixture of ceramics and metals. The material properties are assumed that varying continuously from a top surface ( $z = h/2$ ) to the bottom ( $z = -h/2$ ) surface according to a power-law distribution ( $k$ ). The law of changing the mechanical properties  $P(z)$  through thickness of FGP Beam can be expressed as follows (Houari *et al.* 2018, Shahsavari *et al.* 2018, Tran *et al.* 2021, Selmi 2021, Aalmitani *et al.* 2021)

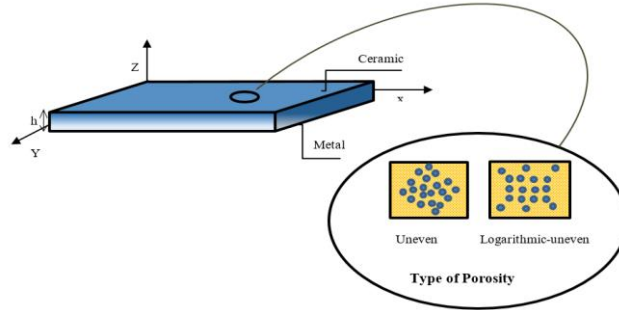


Fig. 1 Model of functionally graded porous beam

$$P(z) = P_m + (P_c - P_m) \left( \frac{1}{2} + \frac{z}{h} \right)^k - \chi(z)(P_c + P_m) \tag{1}$$

Where  $P$  represents material properties such as Young’s modulus  $E$ , mass density  $\rho$ , Poisson’s ratio  $\nu$  and thermal expansion coefficient  $\alpha$ . Subscripts  $c$  and  $m$  denote the ceramic and metal constituents, respectively. The volume fraction of ceramic and metal varying through thickness via the power-law distribution ( $k$ ),  $\chi(z)$  is the coefficient of the porosity distribution and let  $\xi$  be the porosity coefficient.

The relationship between  $\chi(z)$  and  $\xi$  of each type of porosity, distribution is expressed as follows (Shahsavari *et al.* 2018, Tran *et al.* 2021):

- Uneven porosity distribution (uneven)

$$\chi(z) = \frac{\xi}{2} \left( 1 - \frac{2|z|}{h} \right) \tag{2a}$$

- Logarithmic-uneven porosity distribution (Log-uneven)

$$\chi(z) = \left( 1 - \frac{2|z|}{h} \right) \log_{10} \left( \frac{\xi}{2} + 1 \right) \tag{2b}$$

In the present work, we propose two modified models of the porosity distribution through the thickness of the FGP Beam, inspired by the two models proposed by (Shahsavari *et al.* 2018, Tran *et al.* 2021) in Eqs. (2a), (2b) as:

- Uneven porosity distribution (uneven)

$$\chi(z) = \frac{\xi}{2} \left( 1 - \frac{2|z|}{h} \right)^p \tag{3a}$$

- Logarithmic-uneven porosity distribution (Log-uneven)

$$\chi(z) = \left( 1 - \frac{2|z|}{h} \right)^p \log_{10} \left( \frac{\xi}{2} + 1 \right) \tag{3b}$$

Where:  $p$  is the porosity parameter.

The two models proposed above have the advantage of giving several forms of porosity distribution through the thickness of the structure and this for any value of material parameter  $k$ .

The law of changing the mechanical properties  $P(z)$  through thickness of FG beam without

porosity can be easily obtained by setting  $\xi = 0$  in (3), that is

$$P(z) = P_m + (P_c - P_m) \left( \frac{1}{2} + \frac{z}{h} \right)^k \quad (4)$$

## 2.2 Constitutive relations

### 2.2.1 Basic assumptions

The assumptions of the present theory are as follows:

The displacements are small in comparison with the plate thickness and, therefore, strains involved are infinitesimal. The transverse normal stress  $\sigma_z$  is negligible in comparison with in-plane stresses  $\sigma_x$  and  $\sigma_y$ . This theory assumes constant transverse shear stress, and it needs a shear correction factor in order to have deformation energy due to the shear deformation effect equal to that obtained by the exact solution of the elasticity.

### 2.2.2 Kinematics

Based on the assumptions made in the preceding section, the displacement field can be obtained as follows

$$u(x, y) = u_0(x, y) - z \frac{\partial \Phi}{\partial x} \quad (5a)$$

$$v(x, y) = v_0(x, y) - z \frac{\partial \Phi}{\partial y} \quad (5b)$$

$$w(x, y, z) = w_0(x, y) \quad (5c)$$

Where,  $u, v, w$  are displacements in the  $z$  directions,  $u_0$  and  $v_0$  are the mid plane surface displacements,  $\Phi$  is function of coordinates  $x, y$ .

The strains associated with the displacements in Eq. (5) are

$$\begin{Bmatrix} \varepsilon_x \\ \varepsilon_y \\ \gamma_{xy} \end{Bmatrix} = \begin{Bmatrix} \varepsilon_x^0 \\ \varepsilon_y^0 \\ \gamma_{xy}^0 \end{Bmatrix} + z \begin{Bmatrix} k_x \\ k_y \\ k_{xy} \end{Bmatrix}, \quad \begin{Bmatrix} \gamma_{yz} \\ \gamma_{xz} \end{Bmatrix} = \begin{Bmatrix} \gamma_{yz}^s \\ \gamma_{xz}^s \end{Bmatrix} \quad (6)$$

$$\begin{Bmatrix} \varepsilon_x^0 \\ \varepsilon_y^0 \\ \gamma_{xy}^0 \end{Bmatrix} = \begin{Bmatrix} \frac{\partial u_0}{\partial x} \\ \frac{\partial v_0}{\partial x} \\ \frac{\partial u_0}{\partial y} + \frac{\partial v_0}{\partial x} \end{Bmatrix}, \quad \begin{Bmatrix} k_x \\ k_y \\ k_{xy} \end{Bmatrix} = \begin{Bmatrix} -\frac{\partial^2 \Phi}{\partial x^2} \\ -\frac{\partial^2 \Phi}{\partial y^2} \\ -2 \frac{\partial^2 \Phi}{\partial x \partial y} \end{Bmatrix}, \quad \begin{Bmatrix} \gamma_{yz}^s \\ \gamma_{xz}^s \end{Bmatrix} = \begin{Bmatrix} \frac{\partial w}{\partial y} - \frac{\partial \Phi}{\partial y} \\ \frac{\partial w}{\partial x} - \frac{\partial \Phi}{\partial x} \end{Bmatrix} \quad (7)$$

Where

$$\varepsilon_x = \frac{\partial u_0}{\partial x} - z \frac{\partial^2 \Phi}{\partial x^2}, \quad \varepsilon_y = \frac{\partial v_0}{\partial x} - z \frac{\partial^2 \Phi}{\partial y^2}, \quad \varepsilon_{xy} = \frac{\partial u_0}{\partial y} + \frac{\partial v_0}{\partial x} - 2 z \frac{\partial^2 \Phi}{\partial x \partial y} \quad (8a)$$

$$\varepsilon_x = \varepsilon_{x0} + z k_x, \quad \varepsilon_y = \varepsilon_{y0} + z k_y, \quad \varepsilon_{xy} = \varepsilon_{xy0} + z k_{xy} \quad (8b)$$

The stiffness coefficients of a functionally graded beam are derived by appropriately modifying

the stiffness coefficients of a functionally graded plate (FGP Plate), and then, the linear constitutive relations for a FGP Beam, including transverse shear deformation (FSDT), are obtained. The in-plane stress-strain relation can be expressed as follows

$$\begin{Bmatrix} \sigma_x \\ \sigma_y \\ \tau_{xy} \end{Bmatrix} = \begin{bmatrix} Q_{11} & Q_{12} & 0 \\ Q_{12} & Q_{22} & 0 \\ 0 & 0 & Q_{66} \end{bmatrix} \begin{Bmatrix} \varepsilon_x \\ \varepsilon_y \\ \gamma_{xy} \end{Bmatrix} \text{ and } \begin{Bmatrix} \tau_{yz} \\ \tau_{zx} \end{Bmatrix} = \begin{bmatrix} Q_{44} & 0 \\ 0 & Q_{55} \end{bmatrix} \begin{Bmatrix} \gamma_{yz} \\ \gamma_{zx} \end{Bmatrix} \quad (9)$$

where  $(\sigma_x, \sigma_y, \tau_{xy}, \tau_{yz}, \tau_{zx})$  and  $(\varepsilon_x, \varepsilon_y, \gamma_{xy}, \gamma_{yz}, \gamma_{zx})$  are the stress and strain components, respectively.

$Q_{ij}$  are the material constants in the material axes of the layer given as

$$Q_{11} = Q_{22} = \frac{E(z)}{1 - \nu^2} \quad (10a)$$

$$Q_{12} = \frac{\nu E(z)}{1 - \nu^2} \quad (10b)$$

$$Q_{66} = \frac{E(z)}{2(1 + \nu)} \quad (10c)$$

First, we obtain expressions for the axial and bending stress resultants. Using a classical plate theory approach, the integration of stresses, given in Eq. (9), through the thickness of FG plate results in the following relation between the stress resultants and the strains and curvatures

$$\begin{Bmatrix} N \\ M \end{Bmatrix} = \begin{bmatrix} A & B \\ B & D \end{bmatrix} \begin{Bmatrix} \varepsilon \\ k \end{Bmatrix} \quad (11)$$

Where

$$N = \{N_x, N_y, N_{xy}\}^t, \quad M = \{M_x, M_y, M_{xy}\}^t \quad (12a)$$

$$\varepsilon = \{\varepsilon_x^0, \varepsilon_y^0, \gamma_{xy}^0\}^t, \quad k = \{k_x, k_y, k_{xy}\}^t \quad (12b)$$

and the expressions for the stiffness sub-matrices are expressed as follows:

$$\begin{aligned} (A_{11}, B_{11}, D_{11}) &= \int_{-h/2}^{h/2} Q_{11} (1, z, z^2) dz, \quad (A_{12}, B_{12}, D_{12}) = \int_{-h/2}^{h/2} Q_{12} (1, z, z^2) dz, \\ (A_{66}, B_{66}, D_{66}) &= \int_{-h/2}^{h/2} Q_{66} (1, z, z^2) dz \end{aligned} \quad (13)$$

Inversion of the full stiffness matrix in Eq. (11) results in

$$\begin{Bmatrix} [\varepsilon] \\ [k] \end{Bmatrix} = \begin{bmatrix} [\alpha] & [\beta] \\ [\beta] & [\delta] \end{bmatrix} \begin{Bmatrix} [N] \\ [M] \end{Bmatrix} \quad (14)$$

In conformance with the assumptions considered by Whitney *et al.* for obtaining FG beam stiffness coefficients from the equations of the stress resultants of FG beams, the following stress-resultants  $N_y, N_{xy}, M_y,$  and  $M_{xy}$  are equated to zero in Eq. (14) to obtain the compliance coefficients of an FG beam (Whitney *et al.* 1974) as

$$\begin{Bmatrix} \varepsilon_{x0} \\ k_x \end{Bmatrix} = \begin{bmatrix} A & B \\ B & D \end{bmatrix} \begin{Bmatrix} N_x \\ M_x \end{Bmatrix} \quad (15)$$

Inverting Eq. (15) leads to the following expression for the stress-resultants of an FG beam

$$\begin{Bmatrix} N_x \\ M_x \end{Bmatrix} = \begin{bmatrix} \alpha_{11} & \beta_{11} \\ \beta_{11} & \delta_{11} \end{bmatrix} \begin{Bmatrix} \varepsilon_{x0} \\ k_x \end{Bmatrix}$$

where

$$\begin{aligned} A &= \frac{\delta_{11}}{(\alpha_{11}\delta_{11} - \beta_{11}^2)} \\ B &= \frac{\beta_{11}}{(\alpha_{11}\delta_{11} - \beta_{11}^2)} \\ D &= \frac{\alpha_{11}}{(\alpha_{11}\delta_{11} - \beta_{11}^2)} \end{aligned} \quad (16)$$

Next, the transverse shear stress resultant is derived by considering the constitutive relations for transverse shear stresses in an FG plate

$$\begin{Bmatrix} \tau_{yz} \\ \tau_{zx} \end{Bmatrix} = \begin{bmatrix} Q_{44} & 0 \\ 0 & Q_{55} \end{bmatrix} \begin{Bmatrix} \gamma_{yz} \\ \gamma_{zx} \end{Bmatrix} \quad (17)$$

Where

$$Q_{44} = Q_{55} = \frac{E(z)}{2(1 + \nu)} \quad (18)$$

The integration of the transverse shear stresses ( $\tau_{zx}$  and  $\tau_{yz}$  in Eq. (17)) through the thickness of FG plate yields the following relation

$$\begin{Bmatrix} Q_x \\ Q_y \end{Bmatrix} = \begin{bmatrix} k_1^2 A_{44} & 0 \\ 0 & k_2^2 A_{55} \end{bmatrix} \begin{Bmatrix} \gamma_{yz} \\ \gamma_{zx} \end{Bmatrix} \quad (19a)$$

where  $k_1^2$  and  $k_2^2$  are the plate shear correction factors and

$$(A_{44}, A_{55}) = \int_{-h/2}^{h/2} (Q_{44}, Q_{55}) dz \quad (19b)$$

Similar to the assumption considered for the stress resultants due to the in-plane stress components, let  $Q_y = 0$ , and by inversion of the stiffness matrix of Eq. (19), we obtain the constitutive relation for the transverse shear stress resultant of FG beam as

$$\gamma_{xz} = \frac{1}{kF} Q_x \quad (20)$$

Where  $k = k_2^2$  is the shear correction factor and  $F = A_{55}$ .

Thus, from Eqs. (16) and (20) and consistent with FSDT, the constitutive relations of FG beam are expressed as

$$\begin{Bmatrix} N_x \\ M_x \\ Q_x \end{Bmatrix} = \begin{bmatrix} A & B & 0 \\ B & D & 0 \\ 0 & 0 & kF \end{bmatrix} \begin{Bmatrix} \varepsilon_{x0} \\ k_x \\ \gamma_{xz} \end{Bmatrix} \quad (21)$$

### 2.3 Derivation of the shear correction factor

In this section, we extend the theory presented by Bert and Madabhusi-Raman and Davalos to functionally graded beams (Bert 1973, Madabhusi-Raman and Davalos 1996). Using two-dimensional equilibrium equations, an expression is derived for the variation of the transverse

shear stress through the thickness of the FG beam. The shear correction factor is obtained by the following procedure: the shear strain energy, due to transverse shear stress distribution obtained from equilibrium equations, is computed and subsequently equated to the shear strain energy obtained from the constitutive relations for the transverse shear stress resultants of the FG beam given by Eq. (20), which assumes constant transverse shear strain through the thickness of the beam. First, an expression for the transverse shear stress  $\tau_{xz}$  is obtained. The equilibrium equation for the stresses acting in the  $x - z$  plane in the absence of body forces is

$$\sigma_{x,x} + \tau_{xz,z} = 0 \tag{22}$$

Integrating Eq. (22) through the thickness with respect to the  $z$  coordinate, yields

$$\tau_{xz} = - \int_{-h/2}^z \sigma_{x,x} dz \tag{23}$$

Substituting  $\sigma_x$  given in Eq. (9) into Eq. (23), we get

$$\tau_{xz} = - \int_{-h/2}^z \left[ \frac{(Q_{11}\epsilon_{x0} + Q_{12}\epsilon_{y0} + Q_{16}\gamma_{xz0}) + z(Q_{11}\chi_x + Q_{22}\chi_y + Q_{16}\chi_{xy})}{Q_{55}} \right] dz \tag{24}$$

The strains and curvatures in Eq. (24) are replaced by the expressions given in Eq. (14), and considering only the nonzero stress-resultants, Eq. (24) becomes

$$\tau_{xz} = - \int_{-h/2}^z (N_{x,x}(Q_{1i}\alpha_{1i} + zQ_{1i}\beta_{1i}) + M_{x,x}(Q_{1i}\beta_{1i} + zQ_{1i}\delta_{1i})) dz, \text{ for } i = 1,2,6 \tag{25}$$

Using the expressions  $N_{x,x} = 0$  (the case where there is no distributed load in axial direction),  $M_{x,x} = Q_x$  from the resultant equilibrium equations of static beam theory, we have

$$\tau_{xz} = - \int_{-h/2}^z (Q_x(Q_{1i}\beta_{1i} + zQ_{1i}\delta_{1i})) dz, \text{ for } i = 1,2,6 \tag{26}$$

Eq. (26) is the expression for the variation of the transverse shear stress through the thickness. From the constitutive relation for transverse shear given in Eq. (17), the following expression is obtained for the shear strain energy per unit length

$$\bar{U} = \frac{1}{2} \int_{-h/2}^{h/2} \frac{\tau_{xz}^2}{Q_{55}} dz \tag{27}$$

Substituting  $\tau_{xz}$  from Eq. (26) in Eq. (27), the shear strain energy per unit length is expressed as

$$\bar{U} = \frac{1}{2} \int_{-h/2}^{h/2} Q_x^2 \frac{\left[ \int_{-h/2}^z (Q_{1i}\beta_{1i} + zQ_{1i}\delta_{1i}) dz \right]^2}{Q_{55}} dz, \tag{28}$$

Where  $i=1,2,6$

Similarly, the shear strain energy per unit length computed from the constitutive relation of Eq. (20), which assumes constant transverse shear strain, is

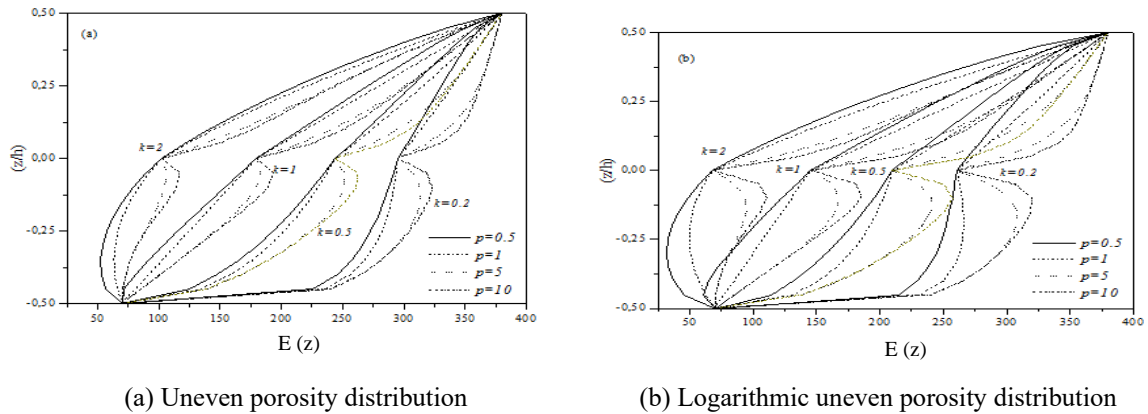


Fig. 2 The Young's modulus  $E(z)$  with different porosity distributions, different values of power law index  $k$  and different values of porosity parameter  $p$

$$\bar{U} = \frac{1}{2k} \frac{Q_x^2}{A_{55}} \quad (29)$$

Equating Eqs. (28) and (29), the expression for the shear correction factor for P-FG beam is given by

$$k = \frac{1}{A_{55}} \left[ \int_{-h/2}^{h/2} \frac{\left[ \int_{-h/2}^z (Q_x(Q_{1i} \beta_{1i} + zQ_{1i} \delta_{1i})) dz \right]^2}{Q_{55}} dz \right]^{-1}, \quad (30)$$

Where  $i=1,2,6$

### 3. Numerical results

A beam consisting of metal and ceramic substances of an FGM is considered as an example. Young's modulus for metal (Aluminium) is  $E_b = 70$  GPa, and for ceramic (SiC) is  $E_t = 380$  GPa. Note that Poisson's ratio is selected constant and equal to 0.3 for both of the constituents. For  $\xi = 0.2$ , Fig. 2 shows that the variation of elastic Young's modulus  $E(z)$  through thickness in  $z$ -axis of functionally graded porous beams for type uneven of porosity distributions (Fig. 2(a)) and the Logarithmic-uneven type (Fig. 2(b)) with different values of power law index  $k$  and different values of porosity parameter  $p$ . It is seen from the above figures that the variation of Young's modulus is continuous for values of the porosity parameter  $p < 1$ ; which gives the same appearance of the graph of the case without porosity (Fig. 3), but the graphs are non-continuous and move towards larger values with an increasing parameter value of porosity, and this for the two forms of porosity distribution. It is clear that Young's modulus decreases with increasing the power law index  $p$  and increase with increasing the porosity parameter  $p$ . Thus, it can be concluded that the presence of pores has a considerable effect on Young's modulus and the more the porosity parameter  $p$  values increase the more the Young's modulus values increase and this for any value of power law index  $k$ .

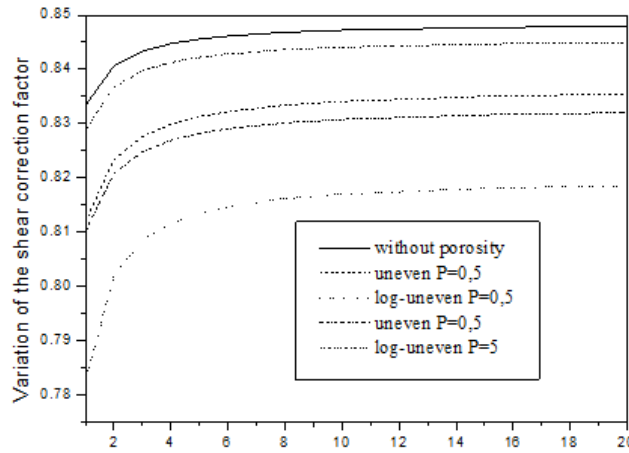


Fig. 4 Comparison of Variation of the shear correction factor for the FG beam without porosity and two types of porosity (uneven, Log-unven) for  $p = 0.5$

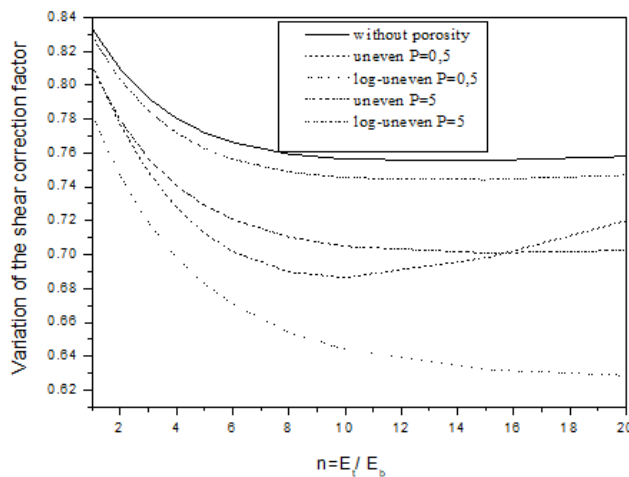


Fig. 5 The variation of Young's modulus with power-law distribution  $k$  without porosity

### 3.1 Shear correction factor for FGP beams

#### 3.1.1 FG beams without porosity ( $\xi = 0.2$ )

Table 1 presents values of shear correction factors for a FG beam without porosity calculated by Eq. (4) they are equal to the values given by Nguyen *et al.* (2008) and Mena *et al.* (2012). The shear correction factors are equal to  $5/6$  as for a homogeneous beam for  $k = 0$  and  $E_t/E_b = 1$  and approximately this usual value for  $k = 1$ . The comparison of Variation of the shear correction factor for the FG beam without porosity and two types of porosity (uneven, Log-unven) for  $k = 0.5$  and  $k = 2$  (Fig. 4 and Fig. 5) confirm the effect of porosity.

#### 3.1.2 Shear correction factor for FGP beams related to couple $(k, n)$

##### 3.1.2.1 Uneven porosity distribution (uneven)

Table 2 Shear correction factors for the FG beams, Uneven porosity distribution  $\xi = 0.2$  (uneven) according to  $n = E_t/E_b$  and the porosity parameter  $p$  and the power law index  $k$

|     |     | New model uneven $\xi = 0.2$ |         |         |         |         |         |         |         |         |         |
|-----|-----|------------------------------|---------|---------|---------|---------|---------|---------|---------|---------|---------|
| $p$ | $k$ | $n = E_t/E_b$                |         |         |         |         |         |         |         |         |         |
|     |     | 1                            | 2       | 3       | 4       | 5       | 6       | 8       | 10      | 15      | 20      |
| 0,5 | 0   | 0,81190                      | 0,81042 | 0,81996 | 0,82896 | 0,82145 | 0,82818 | 0,82078 | 0,82227 | 0,82242 | 0,82254 |
|     | 1   | 0,81190                      | 0,82335 | 0,82763 | 0,82988 | 0,83127 | 0,83221 | 0,83288 | 0,83339 | 0,83378 | 0,83409 |
|     | 5   | 0,81190                      | 0,80973 | 0,80795 | 0,80739 | 0,80752 | 0,80799 | 0,80860 | 0,80925 | 0,80988 | 0,81048 |
|     | 10  | 0,81190                      | 0,77637 | 0,74851 | 0,72769 | 0,71253 | 0,70179 | 0,69447 | 0,68983 | 0,68732 | 0,68649 |
| 1   | 0   | 0,80462                      | 0,81273 | 0,81528 | 0,81653 | 0,81727 | 0,81776 | 0,81810 | 0,81837 | 0,81857 | 0,81873 |
|     | 1   | 0,80462                      | 0,81672 | 0,82128 | 0,82369 | 0,82518 | 0,82619 | 0,82691 | 0,82746 | 0,82789 | 0,82823 |
|     | 5   | 0,80462                      | 0,80256 | 0,80074 | 0,79999 | 0,79988 | 0,80010 | 0,80046 | 0,80089 | 0,80133 | 0,80176 |
|     | 10  | 0,80462                      | 0,76894 | 0,74150 | 0,72099 | 0,70579 | 0,69456 | 0,68632 | 0,68034 | 0,67611 | 0,67323 |
| 10  | 0   | 0,81008                      | 0,81663 | 0,81870 | 0,81971 | 0,82031 | 0,82071 | 0,82099 | 0,82120 | 0,82136 | 0,82149 |
|     | 1   | 0,81855                      | 0,82801 | 0,83155 | 0,83339 | 0,83451 | 0,83525 | 0,83578 | 0,83617 | 0,83648 | 0,83672 |
|     | 5   | 0,81855                      | 0,81715 | 0,81591 | 0,81537 | 0,81523 | 0,81528 | 0,81543 | 0,81562 | 0,81581 | 0,81600 |
|     | 10  | 0,81855                      | 0,79028 | 0,76998 | 0,75561 | 0,74541 | 0,73813 | 0,73293 | 0,72922 | 0,72658 | 0,72474 |

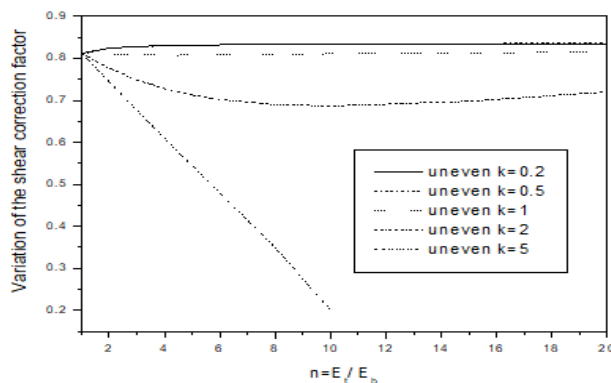


Fig. 6 Variation of the shear correction factor according to  $n = E_t/E_b$  and the power law index  $k$  for the FG beam uneven  $p = 0.5$  and  $\xi = 0.2$

For FGP beam with the uneven porosity distribution (uneven), Table 2, Fig. 6 and Fig. 7 give the values of the shear corrections factors SCF related to every couple  $(k, n)$  with different values of porosity parameter  $p$  calculated by Eq. (1) and Eq. (3a). In the case of  $E_t/E_b = 1$ , the values of the shear corrections factors SCF are close to each other whatever the changes of the variables  $p$  and  $k$  and lower than 5/6 as for  $\xi = 0$  (Fig. 4 and Fig. 5).

- For  $k \leq 1$  we notice a slight variation in the values of SCF;
- For  $k > 1$  SCF decreases as  $n$  increases;

the decrease in the values of the CSF becomes significant from  $k \geq 3$ .

### 3.1.2.2 Logarithmic uneven porosity distribution (log-uneven):

In application of Eq. (1) and Eq. (3b) Table 3, the variation of the shear corrections factors SCF according to  $n$  and  $k$  with different values of porosity parameter  $p$  (Fig. 8, Fig. 9) the

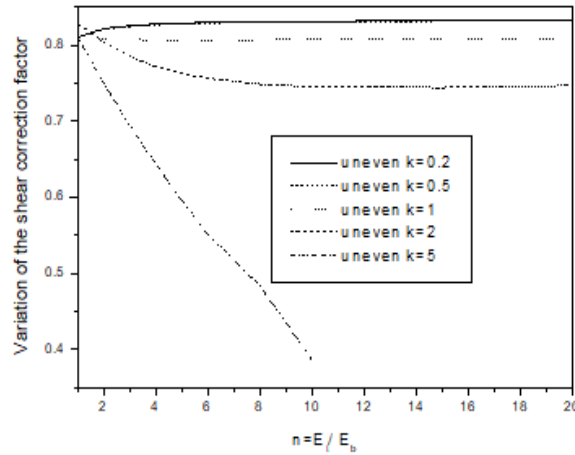


Fig. 7 Variation of the shear correction factor according to  $n = E_t/E_b$  and the power law index  $k$  for the FG beam uneven  $p = 5$  and  $\xi = 0.2$

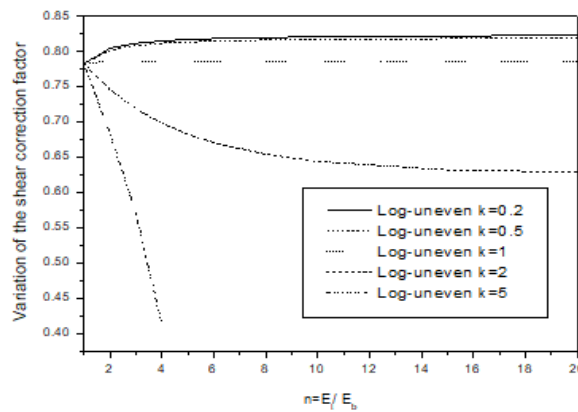


Fig. 8 Variation of the shear correction factor according to  $n = E_t/E_b$  and the power law index  $k$  for the FG beam Log-uneven  $p = 0.5$  and  $\xi = 0.2$

SCF increases with increasing  $n$ , whatever the value of  $p$  or  $k$ .

In the case of  $E_t/E_b = 1$ , the values of the shear corrections factors SCF are close to each other whatever the changes of the variables  $p$  and  $k$  and lower than  $5/6$  as for  $\xi = 0$  (Fig. 4 and Fig. 5).

- For  $k \leq 1$  notice a slight variation in the values of SCF
- For  $k > 1$ , SCF decreases as  $n$  increases.

the decrease in the values of the SCF becomes significant from  $k \geq 3$ .

### 3.1.3 Shear correction factor for FGP beams related to couple $(p, n)$

#### 3.1.3.1 Uneven porosity distribution (uneven)

Table 4 gives the values of the shear corrections factors SCF related to every couple  $(p, n)$  calculated by Eq. (1) and Eq. (3a). Fig. 10 and Fig. 11 show that whatever the value of  $p$ , a very slight variation of SCF Independent of the value of  $n$  and the confirmation of the remarks mentioned above for the couple  $(k, n)$ .

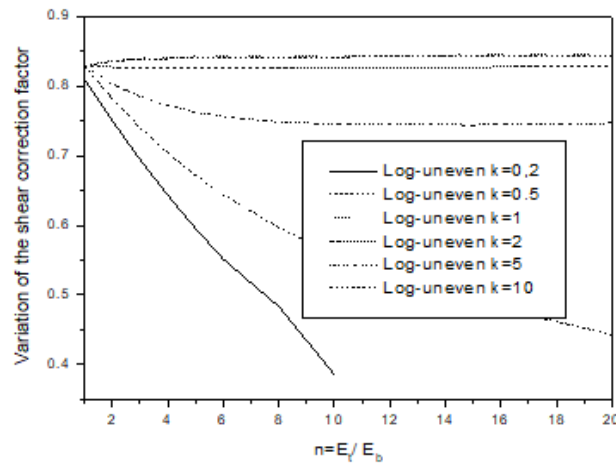


Fig. 9 Variation of the shear correction factor according to  $n = E_t/E_b$  and the power law index  $k$  for the FG beam Log-uneven  $p = 5$  and  $\xi = 0.2$

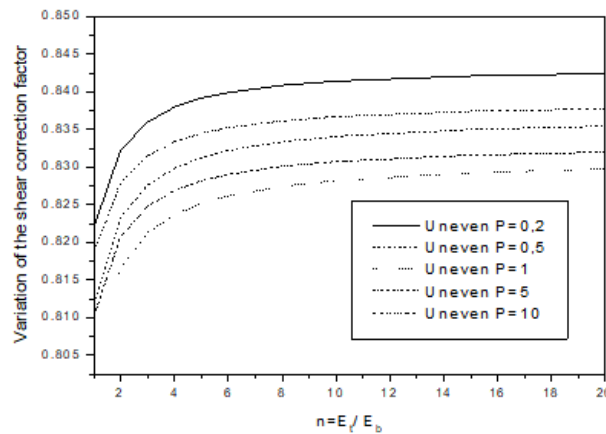


Fig. 10 Variation of the shear correction factor according to  $n = E_t/E_b$  and the porosity parameter  $p$  for the FG beam uneven  $k = 0.5$  and  $\xi = 0.2$

### 3.1.3.2 Logarithmic-uneven porosity distribution (log-uneven):

In application of Eq (1) and Eq (3b) Table 5, Fig. 12 and Fig. 13 show, the variation of the shear:

- For  $p < 1$ ; SCF decreases as  $n$  increases;
- For  $p \geq 1$  we notice a slight variation in the values of SCF.

### 3.2 Effect of type of porosity distribution by comparison of uneven and log-uneven of FGP beam on the shear correction

Table 6 and Figs. 8, 9, 10 and 11 represent the variation of shear correction factor with different values of porosity parameter  $p$  for the ratio of elastic modulus  $E_t/E_b = 4$ , it is observed from these theoretical results that:

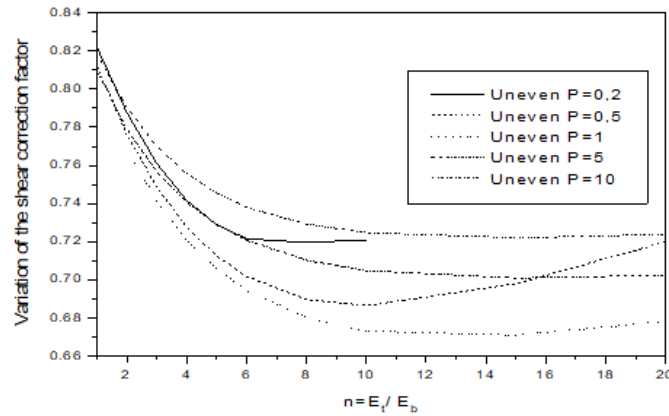


Fig. 11 Variation of the shear correction factor according to  $n = E_t/E_b$  and the porosity parameter  $p$  for the FG beam uneven  $k = 2$  and  $\xi = 0.2$

Table 3 Shear correction factors for the FG beams, Log Uneven porosity distribution  $\xi = 0.2$  according to  $n = E_t/E_b$  and the power law index  $k$

|     |     | New model uneven $\xi = 0.2$ |         |         |         |         |         |         |         |         |         |
|-----|-----|------------------------------|---------|---------|---------|---------|---------|---------|---------|---------|---------|
| $p$ | $k$ | $n = E_t/E_b$                |         |         |         |         |         |         |         |         |         |
|     |     | 1                            | 2       | 3       | 4       | 5       | 6       | 8       | 10      | 15      | 20      |
| 0,5 | 0   | 0,78247                      | 0,80066 | 0,80570 | 0,80806 | 0,80943 | 0,81032 | 0,81094 | 0,81141 | 0,81177 | 0,81205 |
|     | 1   | 0,78247                      | 0,80198 | 0,80847 | 0,81163 | 0,81348 | 0,81468 | 0,81552 | 0,81614 | 0,81661 | 0,81697 |
|     | 5   | 0,78247                      | 0,78619 | 0,78613 | 0,78574 | 0,78544 | 0,78525 | 0,78513 | 0,78506 | 0,78501 | 0,78498 |
|     | 10  | 0,78247                      | 0,74598 | 0,71875 | 0,69824 | 0,68267 | 0,67072 | 0,66145 | 0,65420 | 0,64848 | 0,64396 |
| 1   | 0   | 0,82259                      | 0,82541 | 0,82633 | 0,82678 | 0,82706 | 0,82724 | 0,82737 | 0,82746 | 0,82754 | 0,82760 |
|     | 1   | 0,82259                      | 0,83130 | 0,83498 | 0,83674 | 0,83782 | 0,83854 | 0,83905 | 0,83944 | 0,83973 | 0,83997 |
|     | 5   | 0,82259                      | 0,82103 | 0,81968 | 0,81914 | 0,81906 | 0,81920 | 0,81945 | 0,81973 | 0,82002 | 0,82029 |
|     | 10  | 0,82259                      | 0,79459 | 0,77399 | 0,75919 | 0,74865 | 0,74115 | 0,73585 | 0,73217 | 0,72967 | 0,72806 |
| 10  | 0   | 0,83056                      | 0,83130 | 0,83154 | 0,83165 | 0,83173 | 0,83177 | 0,83181 | 0,83183 | 0,83185 | 0,83187 |
|     | 1   | 0,83056                      | 0,83824 | 0,84110 | 0,84259 | 0,84348 | 0,84408 | 0,84450 | 0,84481 | 0,84505 | 0,84524 |
|     | 5   | 0,83056                      | 0,82916 | 0,82800 | 0,82753 | 0,82744 | 0,82754 | 0,82771 | 0,82792 | 0,82813 | 0,82832 |
|     | 10  | 0,83056                      | 0,80576 | 0,78797 | 0,77547 | 0,76672 | 0,76059 | 0,75631 | 0,75336 | 0,75136 | 0,75007 |

Case when  $k \leq 1$

- For  $p < 1$  SCF decreases as  $n$  increases;
- For  $p \geq 1$ , we notice a slight variation in the values of SCF;

Table 5 and Figs. 14, 15 and 16 represent the variation of shear correction factor with different values of porosity parameter  $P$  for the ratio of elastic modulus  $E_t/E_b = 4$ , it is observed from these theoretical results:

whatever the type of porosity, the variation of SCF remains slight with values exceeding 0.80 for  $k \leq 1$  and the curves of uneven and log-uneven are closer.

For  $k \geq 1$  the variation of the SCF of Log-Uneven porosity distribution has an increasing trend, rough

Table 4 Shear correction factors for the FG beams, Uneven porosity distribution  $\xi = 0.2$ , according to  $n = E_t/E_b$  and  $p$

|     |     | New model uneven $\xi = 0.2$ |         |         |         |         |         |         |         |         |         |
|-----|-----|------------------------------|---------|---------|---------|---------|---------|---------|---------|---------|---------|
| $k$ | $p$ | $n = E_t/E_b$                |         |         |         |         |         |         |         |         |         |
|     |     | 1                            | 2       | 3       | 4       | 5       | 6       | 8       | 10      | 15      | 20      |
| 0,5 | 0,5 | 0,81190                      | 0,82335 | 0,82763 | 0,82988 | 0,83127 | 0,83221 | 0,83288 | 0,83339 | 0,83378 | 0,83409 |
|     | 1   | 0,80462                      | 0,81672 | 0,82128 | 0,82369 | 0,82518 | 0,82619 | 0,82691 | 0,82746 | 0,82789 | 0,82823 |
|     | 5   | 0,81008                      | 0,82078 | 0,82481 | 0,82691 | 0,82819 | 0,82905 | 0,82967 | 0,83012 | 0,83048 | 0,83076 |
|     | 10  | 0,81855                      | 0,82801 | 0,83155 | 0,83339 | 0,83451 | 0,83525 | 0,83578 | 0,83617 | 0,83648 | 0,83672 |
| 0,2 | 0,5 | 0,81190                      | 0,82404 | 0,82812 | 0,83015 | 0,83137 | 0,83217 | 0,83275 | 0,83318 | 0,83351 | 0,83378 |
|     | 1   | 0,80462                      | 0,81807 | 0,82265 | 0,82500 | 0,82633 | 0,82725 | 0,82790 | 0,82840 | 0,82878 | 0,82908 |
|     | 5   | 0,81008                      | 0,82171 | 0,82572 | 0,82775 | 0,82896 | 0,82977 | 0,83035 | 0,83079 | 0,83112 | 0,83139 |
|     | 10  | 0,81855                      | 0,82824 | 0,83157 | 0,83325 | 0,83426 | 0,83494 | 0,83542 | 0,83578 | 0,83606 | 0,83628 |
| 1   | 0,5 | 0,81190                      | 0,80973 | 0,80795 | 0,80739 | 0,80752 | 0,80799 | 0,80860 | 0,80925 | 0,80988 | 0,81048 |
|     | 1   | 0,80462                      | 0,80256 | 0,80074 | 0,79999 | 0,79988 | 0,80010 | 0,80046 | 0,80089 | 0,80133 | 0,80176 |
|     | 5   | 0,81008                      | 0,80856 | 0,80720 | 0,80658 | 0,80640 | 0,80645 | 0,80660 | 0,80680 | 0,80701 | 0,80721 |
|     | 10  | 0,81855                      | 0,81715 | 0,81591 | 0,81537 | 0,81523 | 0,81528 | 0,81543 | 0,81562 | 0,81581 | 0,81600 |
| 2   | 0,5 | 0,81190                      | 0,77637 | 0,74851 | 0,72769 | 0,71253 | 0,70179 | 0,69447 | 0,68983 | 0,68732 | 0,68649 |
|     | 1   | 0,80462                      | 0,76894 | 0,74150 | 0,72099 | 0,70579 | 0,69456 | 0,68632 | 0,68034 | 0,67611 | 0,67323 |
|     | 5   | 0,81008                      | 0,77912 | 0,75668 | 0,74062 | 0,72909 | 0,72075 | 0,71469 | 0,71029 | 0,70711 | 0,70483 |
|     | 10  | 0,81855                      | 0,79028 | 0,76998 | 0,75561 | 0,74541 | 0,73813 | 0,73293 | 0,72922 | 0,72658 | 0,72474 |

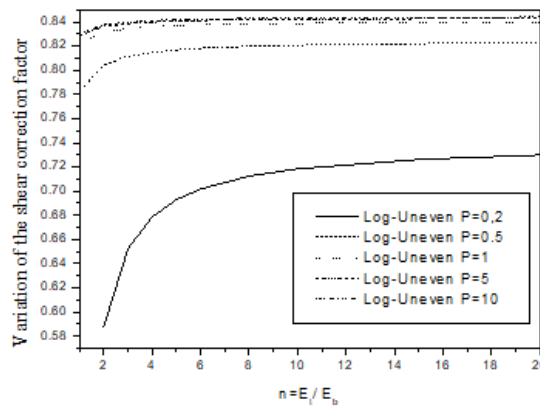


Fig. 12 Variation of the shear correction factor according to  $n = E_t/E_b$  and the porosity parameter  $p$  for the FG beam Log-uneven  $k = 0.5$  and  $\xi = 0.2$

For  $p < 1$  and slow for  $p \geq 1$ .  
 we note for the variation of the SCF of Uneven porosity distribution a decreasing trend for  $p < 1$  and increasing for  $p \geq 1$ .

#### 4. Conclusions

New theoretical formulas for the porosity distribution uneven porosity and logarithmic uneven

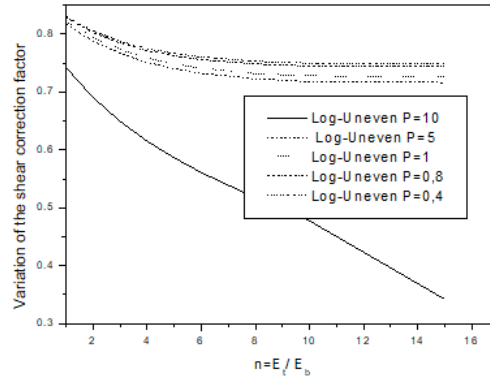


Fig. 13 Variation of the shear correction factor according to  $n = E_t/E_b$  and the porosity parameter  $p$  for the FG beam Log-uneven  $k = 2$  and  $\xi = 0.2$

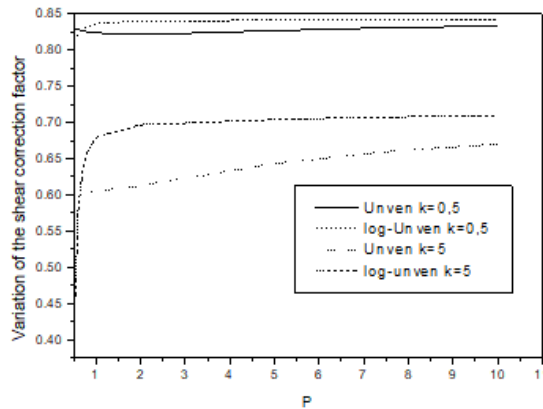


Fig. 14 Effect of the type of porosity distribution uneven and Log-uneven of FGP beam on shear correction for  $E_t/E_b = 4$  and  $\xi = 0.2$

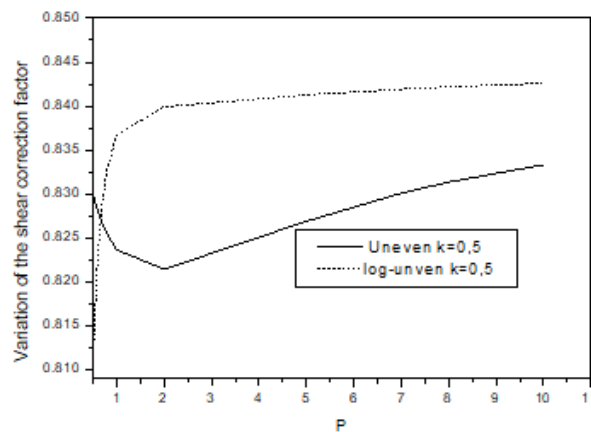


Fig. 15 Effect of the type of porosity distribution uneven and Log-uneven of FGP beam on shear correction for  $E_t/E_b = 4$ ,  $k = 0.5$  and  $\xi = 0.2$

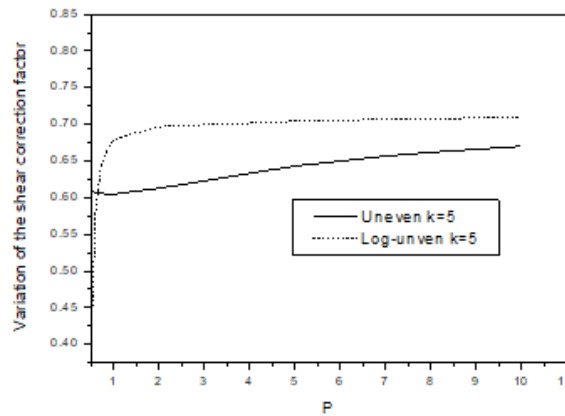


Fig. 16 Effect of the type of porosity distribution uneven and Log-uneven of FGP beam on shear correction for  $E_t/E_b = 4$ ,  $k = 5$  and  $\xi = 0.2$

Table 5 Shear correction factors for the FG beams, log Uneven porosity distribution  $\xi = 0.2$ , according to  $n = E_t/E_b$  and  $p$

|     |     | New model uneven $\xi = 0.2$ |         |         |         |         |         |         |         |         |         |
|-----|-----|------------------------------|---------|---------|---------|---------|---------|---------|---------|---------|---------|
| $k$ | $p$ | $n = E_t/E_b$                |         |         |         |         |         |         |         |         |         |
|     |     | 1                            | 2       | 3       | 4       | 5       | 6       | 8       | 10      | 15      | 20      |
| 0,5 | 0,5 | 0,78247                      | 0,80198 | 0,80847 | 0,81163 | 0,81348 | 0,81468 | 0,81552 | 0,81614 | 0,81661 | 0,81697 |
|     | 1   | 0,82259                      | 0,83130 | 0,83498 | 0,83674 | 0,83782 | 0,83854 | 0,83905 | 0,83944 | 0,83973 | 0,83997 |
|     | 5   | 0,82886                      | 0,83676 | 0,83973 | 0,84128 | 0,84222 | 0,84285 | 0,84330 | 0,84363 | 0,84388 | 0,84408 |
|     | 10  | 0,83056                      | 0,83824 | 0,84110 | 0,84259 | 0,84348 | 0,84408 | 0,84450 | 0,84481 | 0,84505 | 0,84524 |
| 0,2 | 0,5 | 0,78247                      | 0,80465 | 0,81156 | 0,81491 | 0,81689 | 0,81819 | 0,81911 | 0,81980 | 0,82033 | 0,82076 |
|     | 1   | 0,82259                      | 0,83139 | 0,83442 | 0,83595 | 0,83686 | 0,83747 | 0,83791 | 0,83824 | 0,83849 | 0,83869 |
|     | 5   | 0,82886                      | 0,83613 | 0,83865 | 0,83991 | 0,84068 | 0,84118 | 0,84154 | 0,84181 | 0,84202 | 0,84219 |
|     | 10  | 0,83056                      | 0,83744 | 0,83982 | 0,84101 | 0,84173 | 0,84221 | 0,84255 | 0,84280 | 0,84300 | 0,84316 |
| 1   | 0,5 | 0,78247                      | 0,78619 | 0,78613 | 0,78574 | 0,78544 | 0,78525 | 0,78513 | 0,78506 | 0,78501 | 0,78498 |
|     | 1   | 0,82259                      | 0,82103 | 0,81968 | 0,81914 | 0,81906 | 0,81920 | 0,81945 | 0,81973 | 0,82002 | 0,82029 |
|     | 5   | 0,82886                      | 0,82730 | 0,82609 | 0,82561 | 0,82554 | 0,82566 | 0,82586 | 0,82609 | 0,82632 | 0,82655 |
|     | 10  | 0,83056                      | 0,82916 | 0,82800 | 0,82753 | 0,82744 | 0,82754 | 0,82771 | 0,82792 | 0,82813 | 0,82832 |
| 2   | 0,5 | 0,78247                      | 0,74598 | 0,71875 | 0,69824 | 0,68267 | 0,67072 | 0,66145 | 0,65420 | 0,64848 | 0,64396 |
|     | 1   | 0,82259                      | 0,79459 | 0,77399 | 0,75919 | 0,74865 | 0,74115 | 0,73585 | 0,73217 | 0,72967 | 0,72806 |
|     | 5   | 0,82886                      | 0,80327 | 0,78483 | 0,77184 | 0,76272 | 0,75633 | 0,75184 | 0,74874 | 0,74664 | 0,74527 |
|     | 10  | 0,83056                      | 0,80576 | 0,78797 | 0,77547 | 0,76672 | 0,76059 | 0,75631 | 0,75336 | 0,75136 | 0,75007 |

are developed by using the reduced number of unknowns of the theory of FSDT, the energy equivalence principle and equation for the shear correction factor; some conclusions from numerical investigations are given as follows:

- The presence of pores has a considerable effect on Young’s modulus for any value of power law index  $k$ .
- The law of a changing the mechanical properties  $p = (k)$  through the thickness of FG beam without porosity is valeted.

Table 6 Shear correction factors for the FG beams without porosity

| $p$ | $k = 0.5$ |            | $k = 5$ |            |
|-----|-----------|------------|---------|------------|
|     | Uneven    | Log uneven | Uneven  | Log uneven |
| 0,5 | 0,82988   | 0,81163    | 0,60924 | 0,41217    |
| 0,6 | 0,82810   | 0,82292    | 0,60726 | 0,58217    |
| 0,7 | 0,82663   | 0,82922    | 0,60597 | 0,63432    |
| 0,8 | 0,82544   | 0,83295    | 0,60521 | 0,65866    |
| 1   | 0,82369   | 0,83674    | 0,60486 | 0,67977    |
| 2   | 0,82146   | 0,83993    | 0,61283 | 0,69684    |
| 5   | 0,82691   | 0,84128    | 0,64320 | 0,70412    |
| 7   | 0,83011   | 0,84193    | 0,65663 | 0,70680    |
| 8   | 0,83137   | 0,84219    | 0,66182 | 0,70780    |
| 10  | 0,83333   | 0,84259    | 0,67004 | 0,70934    |

- For  $k = 0$  and  $E_t/E_b = 1$ , the shear correction factors are equal to  $5/6$  and substantially of the same value for  $k = 1$ ; Which differs from the case where we consider the porosity ( $\xi \neq 0$ ).
- For both cases, uneven (UNEVEN) and Logarithmic uneven (LOG-UNEVEN) porosity distribution, with increasing  $n$ , the values of the shear correction factors SCF related to every couple  $(p, n)$  increase for the power law index  $k < 1$ , and decrease for  $k \geq 1$ .
- For  $E_t/E_b = 1$ , the values of the shear correction factors SCF are close to each other and lower than  $5/6$  for  $p = 0$  with the difference in the log- uneven porosity distribution (log-uneven), the values are dependent on the variables  $p$  and independent of the variables  $k$  which once again confirms the effect of porosity. The present analytical solution based on FSDT for porous FGM beam can be used as a reference for future studies.

Finally, the formulation lends itself particularly well to study several problems related to the bending, vibration and dynamic behavior of advanced composite macro/nanostructures subjected to moving loads (Esen 2013, 2015, Esen *et al.* 2018, Esen 2019, 2020, Esen *et al.* 2020, Özarpa and Esen 2020, Gao *et al.* 2020, Qin *et al.* 2019, Qin *et al.* 2020). And for study the other modified continuum theories such as nonlocal strain gradient, modified couple stress, surface energy (Abdelrahman *et al.* 2021a, b, Esen *et al.* 2021, Liu *et al.* 2021a, Liu *et al.* 2022b).

## References

- Abdelrahman, A.A., Esen, I., Özarpa, C. and Eltaher, M.A. (2021a), “Dynamics of perforated nanobeams subject to moving mass using the nonlocal strain gradient theory”, *Appl. Math. Model.*, **96**, 215-235. <http://doi.org/10.1016/j.apm.2021.03.008>.
- Abdelrahman, A.A., Esen, I., Ozarpa, C., Shaltout, R., Eltaher, M.A. and Assie, A.E. (2021b), “Dynamics of perforated higher order nanobeams subject to moving load using the nonlocal strain gradient theory”, *Smart Struct. Syst.*, **28**(4), 515-533. <http://doi.org/10.1016/j.apm.2021.03.008>.
- Abrate, S. (2006), “Free vibration, buckling, and static deflections of functionally graded plates”, *Compos. Sci. Technol.*, **66**, 2383-2394. <http://doi.org/10.1016/j.compscitech.2006.02.032>.
- Almitani, K.H., Eltaher, M.A., Abdelrahman, A.A. and Abd-El-Mottaleb, H.E. (2021), “Finite element based stress and vibration analysis of axially functionally graded rotating beams”, *Struct. Eng. Mech.*, **79**(1), 23-33. <https://doi.org/10.12989/sem.2021.79.1.023>.

- Bert, C.W. (1973), "Simplified analysis of static shear factors for beams of nonhomogeneous cross-section", *J. Compos. Mater.*, **7**, 525. <http://doi.org/10.1177/002199837300700410>.
- Bert, C.W. and Gordaninejad, F. (1983), "Transverse shear effects in bimodular composite laminates", *J. Compos. Mater.*, **17**, 282. [http://doi.org/10.1007/978-3-642-58092-5\\_11](http://doi.org/10.1007/978-3-642-58092-5_11).
- Berthelot, J.M. (1992), *Materiaux Composites*, Comportement Mécanique et Analyse des Structures, Masson, Paris.
- Bever; M.B. and Duwez, P.F. (1972), "Gradients in composite materials", *Mater. Sci. Eng.*, **10**, 1-8. [https://doi.org/10.1016/0025-5416\(72\)90059-6](https://doi.org/10.1016/0025-5416(72)90059-6).
- Birman, V. and Bert, C.W. (2002), "On the choice of shear correction factor in sandwich structures", *J. Sandw. Struct. Mater.*, **4**, 83. <https://doi.org/10.1177/1099636202004001180>.
- Chen, D., Yang, J. and Kitipornchai, S. (2015), "Elastic buckling and static bending of shear deformable functionally graded porous beam", *Compos. Struct.*, **133**, 54-61. <http://doi.org/10.1016/j.compstruct.2015.07.052>.
- Demirhan, P.A. and Taskin, V. (2019), "Bending and free vibration analysis of Levy-type porous functionally graded plate using state space approach", *Compos. B Eng.*, **160**, 661-676. <http://doi.org/10.1016/j.compositesb.2018.12.020>.
- Efraim, E. and Eisenberger, M. (2007), "Exact vibration analysis of variable thickness thick annular isotropic and FGM plates", *J. Sound Vib.*, **299**, 720-738. <http://doi.org/10.1016/j.jsv.2006.06.068>.
- Esen, I. (2013), "A new finite element for transverse vibration of rectangular thin plates under a moving mass", *Finite Elem. Anal. Des.*, **66**, 26-35. <http://doi.org/10.1016/j.finel.2012.11.005>.
- Esen, İ. (2015), "A new FEM procedure for transverse and longitudinal vibration analysis of thin rectangular plates subjected to a variable velocity moving load along an arbitrary trajectory", *Lat. Am. J. Solid. Struct.*, **12**, 808-830. <http://doi.org/10.1590/1679-78251525>.
- Esen, I. (2019), "Dynamic response of a functionally graded Timoshenko beam on two-parameter elastic foundations due to a variable velocity moving mass", *Int. J. Mech. Sci.*, **153**, 21-35. <http://doi.org/10.1016/j.ijmecsci.2019.01.033>.
- Esen, I. (2020), "Dynamics of size-dependant Timoshenko micro beams subjected to moving loads. *Int. J. Mech. Sci.*, **175**, 105501. <https://doi.org/10.1016/j.ijmecsci.2020.105501>.
- Esen, I., Abdelrahman, A.A. and Eltahir, M.A. (2020), "Dynamics analysis of timoshenko perforated microbeams under moving loads", *Eng. Comput.*, 1-17. <https://doi.org/10.1007/s00366-020-01212-7>.
- Esen, I., Abdelrahman, A.A. and Eltahir, M.A. (2021), "On vibration of sigmoid/symmetric functionally graded nonlocal strain gradient nanobeams under moving load", *Int. J. Mech. Mater. Des.*, **17**(3), 721-742. <http://doi.org/10.1007/s10999-021-09555-9>.
- Esen, I., Koc, M.A. and Cay, Y. (2018), "Finite element formulation and analysis of a functionally graded Timoshenko beam subjected to an accelerating mass including inertial effects of the mass", *Lat. Am. J. Solid. Struct.*, **15**(10), 1. <http://doi.org/10.1590/1679-78255102>.
- Ferreira, A.J.M., Batra, R.C., Roque, C.M.C., Qian, L.F. and Jorge, R.M.N. (2006), "Natural frequencies of functionally graded plates by a meshless method", *Compos. Struct.*, **75**, 593-600. <https://doi.org/10.1016/j.compstruct.2006.04.018>.
- Gao, W., Qin, Z. and Chu, F. (2020), "Wave propagation in functionally graded porous plates reinforced with graphene platelets", *Aerosp. Sci. Technol.*, **102**, 105860. <https://doi.org/10.1016/j.ast.2020.105860>.
- Goetzl, C.G. and Lavendel, H.W. (1964), "Multiple scale analysis of heterogeneous elastic structures using homogenization theory and Voronoi cell finite element method", *Int. J. Solid. Struct.*, **32**, 149-162. [https://doi.org/10.1016/0020-7683\(94\)00097-G](https://doi.org/10.1016/0020-7683(94)00097-G).
- Houari, M.S.A., Bessaim, A., Bernard, F., Tounsi, A. and Mahmoud, S.R. (2018), "Buckling analysis of new quasi-3D FG nanobeams based on nonlocal strain gradient elasticity theory and variable length scale parameter", *Steel Compos. Struct.*, **28**(1), 13-24. <https://doi.org/10.12989/scs.2018.28.1.013>.
- Jalali, M.H., Zargar, O. and Baghani, M. (2019), "Size-dependent vibration analysis of fg microbeams in thermal environment based on modified couple stress theory", *Iran. J. Sci. Technol.-Trans. Mech. Eng.*, **43**(s1), 761-771. <http://doi.org/10.1007/s40997-018-0193-6>.
- Koizumi, M. (1997), "FGM activities in Japan", *Compos. Part B*, **28**, 1-4. <https://doi.org/10.1016/S1359->

- 8368(96)00016-9.
- Liu, Y., Qin, Z. and Chu, F. (2021a), "Nonlinear dynamic responses of sandwich functionally graded porous cylindrical shells embedded in elastic media under 1: 1 internal resonance", *Appl. Math. Mech.*, **42**(6), 805-818. <https://doi.org/10.1007/s10483-021-2740-7>.
- Liu, Y., Qin, Z. and Chu, F. (2021b), "Nonlinear forced vibrations of FGM sandwich cylindrical shells with porosities on an elastic substrate", *Nonlin. Dyn.*, **104**, 1007-1021. <https://doi.org/10.1007/s11071-021-06358-7>.
- Liu, Y., Qin, Z. and Chu, F. (2022), "Analytical study of the impact response of shear deformable sandwich cylindrical shell with a functionally graded porous core", *Mech. Adv. Mater. Struct.*, **29**(9), 1338-1347. <https://doi.org/10.1080/15376494.2020.1818904>.
- Madabhusi-Raman, P. and Davalos, J.F. (1996), "Static shear correction factor for laminated rectangular beams", *Compos. Part B: Eng.*, **27**, 285-293. [https://doi.org/10.1016/1359-8368\(95\)00014-3](https://doi.org/10.1016/1359-8368(95)00014-3).
- Menaa, R., Tounsi, A., Mouaici, F., Mechab, I., Zidi, M. and Bedia, A. (2012), "Analytical solutions for static shear correction factor of functionally graded rectangular beams", *Mech. Adv. Mater. Struct.*, **19**, 641-652. <https://doi.org/10.1080/15376494.2011.581409>.
- Mortensen, A. and Suresh, S. (1998), *Fundamentals of Functionally Graded Materials: Processing and Thermomechanical Behaviour of Graded Metals and Metal-ceramic Composites*, Maney Publishing.
- Mouaici, F., Benyoucef, S., Ait Atmane, H. and Tounsi, A. (2016), "Effect of porosity on vibrational characteristics of non-homogeneous plates using hyperbolic shear deformation theory", *Wind Struct.*, **22**(4), 429-454. <https://doi.org/10.12989/was.2016.22.4.429>.
- Nguyen, T.K., Sab, K. and Bonnet, G. (2006), "Reissner-Mindlin model for functionally graded materials", *Proc. of 3th European conf on Computational Mechanics*, Lisbon, 6-2006.
- Nguyen, T.K., Sab, K. and Bonnet, G. (2008), "First-order shear deformation plate models for functionally graded materials", *Compos. Struct.*, **83**, 25-36. <https://doi.org/10.1016/j.compstruct.2007.03.004>.
- Noor A.K. and W.S. Burton. (1990), "Assessment of computational models for multilayered anisotropic plates", *Compos. Struct.*, **14**, 233-265. [https://doi.org/10.1016/0263-8223\(90\)90050-O](https://doi.org/10.1016/0263-8223(90)90050-O).
- Noor, A.K. and Burton, W.S. (1989), "Assessment of shear deformation theories for multilayered composite plates", *Appl. Mech. Rev.*, **42**, 1-13. <https://doi.org/10.1115/1.3152418>.
- Noor, A.K. and Burton, W.S. (1989), "Stress and free vibration analyses of multilayered composite plates", *Compos. Struct.*, **11**, 183-204. [http://doi.org/10.1016/0263-8223\(89\)90058-5](http://doi.org/10.1016/0263-8223(89)90058-5).
- Noor, A.K., Burton, W.S. and Peters, J.M. (1990), "Predictor-corrector procedure for stress and free vibration analyses of multilayered composite plates and shells", *Comput. Mech. Appl. Mech. Eng.*, **82**, 341-364. [https://doi.org/10.1016/0045-7825\(90\)90171-H](https://doi.org/10.1016/0045-7825(90)90171-H).
- Qin, Z., Pang, X., Safaei, B. and Chu, F. (2019), "Free vibration analysis of rotating functionally graded CNT reinforced composite cylindrical shells with arbitrary boundary conditions", *Compos. Struct.*, **220**, 847-860. <https://doi.org/10.1016/j.compstruct.2019.04.046>.
- Qin, Z., Zhao, S., Pang, X., Safaei, B. and Chu, F. (2020), "A unified solution for vibration analysis of laminated functionally graded shallow shells reinforced by graphene with general boundary conditions", *Int. J. Mech. Sci.*, **170**, 105341. <https://doi.org/10.1016/j.ijmecsci.2019.105341>.
- Reddy, J.N. (2002), *Energy Principles and Variational Methods in Applied Mechanics*, Wiley, New York.
- Rezaei, A.S. and Saidi, A.R. (2015), "Exact solution for free vibration of thick rectangular plates made of porous materials", *Compos. Struct.*, **134**, 1051-1060. <http://doi.org/10.1016/j.compstruct.2015.08.125>.
- Rezaei, A.S. and Saidi, A.R. (2016), "Application of Carrera unified formulation to study the effect of porosity on natural frequencies of thick porous-cellular plates", *Compos. B Eng.*, **91**, 361-370. <http://doi.org/10.1016/j.compositesb.2015.12.050>.
- Rezaei, A.S. and Saidi, A.R. (2017), "Buckling response of moderately thick fluid-infiltrated porous annular sector plates", *Acta Mechanica*, **228**, 3929-3945. <http://doi.org/10.1007/s00707-017-1908-2>.
- Rezaei, A.S. and Saidi, A.R. (2017), "On the effect of coupled solid-fluid deformation on natural frequencies of fluid saturated porous plates", *Eur. J. Mech. Solid.*, **63**, 99-109. <http://doi.org/10.1016/j.euromechsol.2016.12.006>.
- Sadoun, M., Houari, M.S.A., Bakora, A., Tounsi, A., Mahmoud, S.R. and Alwabli, A.S. (2018), "Vibration

- analysis of thick orthotropic plates using quasi 3D sinusoidal shear deformation theory”, *Geomech. Eng.*, **16**(2), 141-150. <https://doi.org/10.12989/gae.2018.16.2.141>.
- Sadoune, M., Tounsi, A. and Houari, M.S.A. (2014), “A novel first-order shear deformation theory for laminated composite plates”, *Steel Compos. Struct.*, **17**(3), 321-331. <https://doi.org/10.12989/scs.2014.17.3.1321>.
- Safaei, B., Moradi-Dastjerdi, R., Behdinan, K., Qin, Z. and Chu, F. (2019), “Thermoelastic behavior of sandwich plates with porous polymeric core and CNT clusters/polymer nanocomposite layers”, *Compos. Struct.*, **226**, 111209. <http://doi.org/10.1016/j.compstruct.2019.111209>.
- Saidi, H. and Sahla, M. (2019), “Vibration analysis of functionally graded plates with porosity composed of a mixture of Aluminum (Al) and Alumina (Al<sub>2</sub>O<sub>3</sub>) embedded in an elastic medium”, *Frattura ed Integrità Strutturale*, **50**, 286-299. <http://doi.org/10.3221/IGF-ESIS.50.24>.
- Selmi, A. (2021), “Vibration behavior of bi-dimensional functionally graded beams”, *Struct. Eng. Mech.*, **77**(5), 587-599. <https://doi.org/10.12989/sem.2021.77.5.587>.
- Shahsavari, D., Karami, B., Fahham, H.R. and Li, L. (2018), “On the shear buckling of porous nanoplates using a new size-dependent quasi-3D shear deformation theory”, *Acta Mechanica*, **229**(11), 4549-4573. <https://doi.org/10.1007/s00707-018-2247-7>.
- Singh, S.J. and Harsha, S.P. (2020), “Thermo-mechanical analysis of porous sandwich S-FGM plate for different boundary conditions using Galerkin Vlasov’s method, a semi analytical approach”, *Thin Wall. Struct.*, **150**, 106668. <http://doi.org/10.1016/j.tws.2020.106668>.
- Slimane, M., Samir, B., Hakima, B. and Adda, H.M. (2019), “Free vibration analysis of functionally”, *Int. J. Eng. Tech. Res.*, **8**(03), 143. <http://doi.org/10.17577/IJERTV8IS030098>.
- Timoshenko, S.P. (1922), “On the transverse vibrations of bars of uniform cross section”, *Philos. Mag.*, **43**, 125-131. <https://doi.org/10.1080/14786442208633855>.
- Tran, T.T., Van Ke Tran, V.K., Pham, Q.H. and Zenkour, A.M. (2021), “Extended four-unknown higher-order shear deformation nonlocal theory for bending, buckling and free vibration of functionally graded porous nanoshell resting on elastic foundation”, *Compos. Struct.*, **264**, 2-3. <https://doi.org/10.1016/j.compstruct.113737>.
- Vlachoutsis, S. (1992), “Shear correction factors for plates and shells”, *Int. J. Numer. Meth. Eng.*, **33**, 1537-1552. <https://doi.org/10.1002/nme.1620330712>.
- Wang, Y.Q. and Zu, J.W. (2017), “Large-amplitude vibration of sigmoid functionally graded thin plates with porosities”, *Thin Wall. Struct.*, **119**, 911-924. <http://doi.org/10.1016/j.tws.08.012>.
- Wattanasakulpong, N. and Ungbhakorn, V. (2014), “Linear and nonlinear vibration analysis of elastically restrained ends FGM beams with porosities”, *Aerosp. Sci. Technol.*, **32**(1), 111-120. <https://doi.org/10.1016/j.ast.2013.12.002>.
- Whitney, J.M. (1973), “Shear correction factors for orthotropic laminates under static load”, *J. Appl. Mech.*, **40**, 302-1973.
- Whitney, J.M., Browning, C.E. and Mair, A. (1974), “Analysis of the flexure test for laminated composite materials”, *Composite Materials: Testing and Design (Third Conference), ASTM STP*, **546**, 30.
- Yas, M.H. and Rahimi, S. (2020), “Thermal buckling analysis of porous functionally graded nanocomposite beams reinforced by graphene platelets using generalized differential quadrature method”, *Aerosp Sci Technol.*, **107**, 106261. <https://doi.org/10.1016/j.ast.2020.106261>.
- Zenkour, A.M. (2018), “A quasi-3D refined theory for functionally graded single-layered and sandwich plates with porosities”, *Compos. Struct.*, **201**, 38-48. <http://doi.org/10.1016/j.compstruct.05.147>.
- Zhao, X., Lee, Y.Y. and Liew, K.M. (2009), “Free vibration analysis of functionally graded plates using the element-free kp-Ritz method”, *J. Sound Vib.*, **319**, 918-939. <https://doi.org/10.1016/j.jsv.2008.06.025>.